

Kinetic planar resonators from strongly disordered ultra-thin MoC superconducting films investigated by transmission line spectroscopy

M. Baránek,¹ P. Neilinger,^{1, a)} D. Manca,¹ and M. Grajcar^{1, b)}

Department of Experimental Physics, Comenius University, SK-84248 Bratislava, Slovakia

(Dated: 1 March 2021)

The non-contact broadband transmission line flip-chip spectroscopy technique is utilized to probe resonances of mm-sized square kinetic planar resonators made from strongly disordered molybdenum carbide films, in the GHz frequency range. The temperature dependence of the resonances was analyzed by the complex conductivity of disordered superconductor, as proposed in Ref. 1, which involves the Dynes superconducting density of states. The obtained Dynes broadening parameters relate reasonably to the ones estimated from scanning tunneling spectroscopy measurements. The eigenmodes of the kinetic planar 2D resonator were visualized by EM model in Sonnet software. The proper understanding of the nature of these resonances can help to eliminate them, or utilize them e.g. as filters.

Thin disordered superconducting films find a variety of applications in advanced technologies, such as superconducting single-photon detectors,² parametric amplifiers,^{3,4} superinductors,^{5,6} and superconducting quantum bits.⁷ These devices make use of the distinctively high sheet resistance R_s of these films and thus the high kinetic sheet inductance, which is approximately related to R_s and the superconducting energy gap Δ by $L_k = \hbar R_s / \pi \Delta$ at temperatures well below the superconducting critical temperature T_c . These devices typically operate in the GHz frequency range, and the knowledge of their complex conductivity is of crucial importance for the device design and properties. Moreover, the electrodynamic response of these films provides important insight into the fundamental topics of superconductivity, such as the superconductor-insulator quantum phase transition⁸ and the Berezinskii-Kosterlitz-Thouless transition.⁹ To probe the complex conductivity of thin films, either as surface impedance or through penetration depth measurements, several microwave spectroscopy techniques are exploited. These are either narrowband techniques, such as cavity resonators,^{10,11} the parallel plate resonator technique (which is commonly employed to study high- T_c superconductive films), planar transmission line resonators,¹² or broadband spectroscopy techniques like the transmission line or Corbino spectroscopy.^{13–16} The complex conductivity of superconductors is often studied in the vicinity of the superconducting transition.^{17,18} In several cases, resonances in the spectra were reported for metallic and superconducting films on dielectric substrates.^{15,16,19–24} In general, the presence of these resonances is undesirable as they can strongly limit the upper frequency range of the spectroscopy. The origin of these resonances in thin metallic films on a dielectric sample was unveiled by simulations and experiments as substrate and cavity resonances²⁵ and analyzed in detail by neglecting the metallic films.

In this letter, we report on resonances present in the transmission spectra of disordered superconducting films of

molybdenum carbide (MoC) measured by broadband transmission line spectroscopy in temperature range from T_c down to ≈ 500 mK and frequency range from 1 GHz to 16 GHz. The measurements were carried out in flip-chip geometry. The 5 nm thin films with different R_s were sputtered on sapphire substrate and placed on top of the transmission line facing the center conductor. The present resonances are explained by referring them to eigenmodes of a kinetic planar 2D resonator. Low resonance frequencies of the resonator are the result of the high kinetic inductance of the strongly disordered MoC films. Moreover, in contrast to the aforementioned works, we utilize these resonances to determine the Dynes broadening parameter Γ of these films, which is usually determined by scanning tunneling spectroscopy (STS) at temperatures well below T_c . The superconducting density of states (SDOS) of disordered superconductors is characterized by the smearing of coherence peaks and the presence of in-gap states. Their STS spectra are generally analyzed in terms of the Dynes SDOS²⁶ $N(E) = \text{Re}\{(E + i\Gamma) / [(E + i\Gamma)^2 - \Delta^2]^{1/2}\}$. A thorough study of the STS spectra of highly disordered MoC films is presented in Ref. 27. As a result of disorder, the temperature and frequency dependent complex conductivity $\sigma = \sigma_1 - i\sigma_2$ deviates from the well known Mattis-Bardeen conductivity,^{1,28,29} in contrast to clean BCS superconductors. These deviations were directly related to the complex conductivity of disordered superconductors¹ utilizing Nam's theory.³⁰ This approach was furthered to the optical conductivity of disordered superconductors.³¹

A series of four MoC films was sputtered by means of reactive magnetron deposition from a molybdenum target, in argon-acetylene atmosphere on top of 5×5 mm c-cut sapphire substrate. The R_s of the MoC film was subsequently increased by measuring the carbon content, controlled via the argon-acetylene flow in the chamber during the deposition.²⁴ The increased disorder results in increased R_s and the suppression of T_c . Eventually, at critical R_s , these films undergo a superconductor-insulator transition.³² The properties of the samples are listed in the Table I. R_s is measured by Van der Pauw method at room temperature. As the transition of highly disordered superconductors, measured by the DC transport, is broadened, the maximum of the resistivity temperature derivative T_c^{DC} is listed.

Next, the samples were measured by broadband non-

^{a)} Also at Institute of Physics, Slovak Academy of Sciences, Dúbravská cesta, Bratislava, Slovakia.; Electronic mail: pavel.neilinger@fmph.uniba.sk

^{b)} Also at Institute of Physics, Slovak Academy of Sciences, Dúbravská cesta, Bratislava, Slovakia.

TABLE I: Sample parameters: R_s is sheet resistance at room temperature, T_c^{DC} is superconducting critical temperature from transport measurement, T_c^{spec} , Γ^{spec} , and Γ^{STS} are values estimated from spectroscopic measurement in the GHz frequency range and from STS measurements, respectively.

Sample	R_s (Ω)	T_c^{DC} (K)	T_c^{spec} (K)	Γ^{spec}/Δ_0	Γ^{STS}/Δ_0
A	120	7.89	-	-	0
B	212	7.04	7.02	0	0.03
C	565	4.85	5.11	0.2	0.20
D	974	2.44	2.52	0.5	0.44

contact flip-chip transmission line spectroscopic technique, where the sample is placed on top of the transmission line facing the center conductor. The model and the experimental transmission line are shown in Fig. 1.

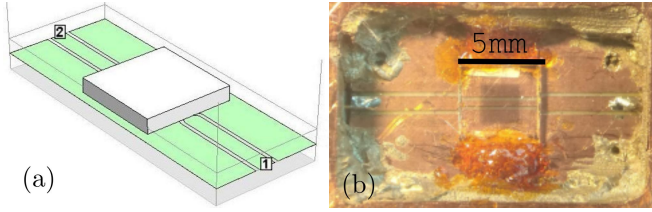


FIG. 1: (Color online) (a) The 3D model of the coplanar waveguide created in SONNET software. The superconducting film is at the bottom of the sapphire substrate. (b) Photo of a rectangular film sample suspended above the transmission line.

The coplanar waveguide was fabricated on a Rogers RO4003 PCB. The tapering in the middle of the transmission line ensures impedance matching upon placing a bare 5×5 mm² sapphire substrate with thickness 460 μ m above the tapering. The bandwidth of the transmission line is up to 18 GHz. The transmission line was fixed to a copper box by silver epoxy and soldered to a SMA Through Hole connector. To ensure electrical insulation, the sample was placed on a thin cigarette paper and fixed by Ge-varnish. The temperature dependence measurements were carried out in a ³He refrigerator and the transmission spectrum was measured by a vector network analyzer, see Fig 2a. Whereas the transmission spectra of sample A with the lowest R_s show the expected step-like increase in the transmission below T_c , the temperature dependence of the spectra for sample B with $R_s=212\Omega$ is slightly disturbed by unexpected resonances close to T_c . The frequency of these resonances increases with decreasing temperature, indicating their dependence on the superconducting properties of the film. Further, these resonances gain in strength and shift to lower frequencies with the increase of R_s , following the $L_k = \hbar R_s / \pi \Delta$ dependence, suggesting their origin in the resonances of the superconducting film.

To further prove this assumption, samples C and D were shaped by optical lithography and dry etching process onto a square with 2.25 mm sidelength. Indeed, this resulted in the increase of the frequencies co-responding to the geomet-

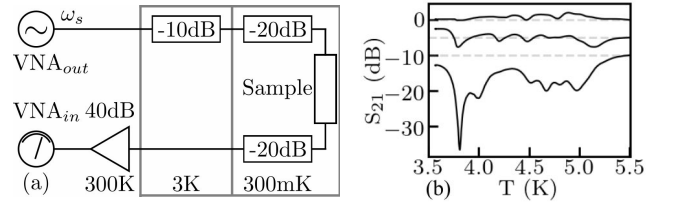


FIG. 2: (a) The scheme of the experimental set-up for transmission measurement. (b) Temperature dependence of the normalized transmission spectra from top to bottom, at 3, 6 and 9 GHz of sample C. The curves are offset by -5dB.

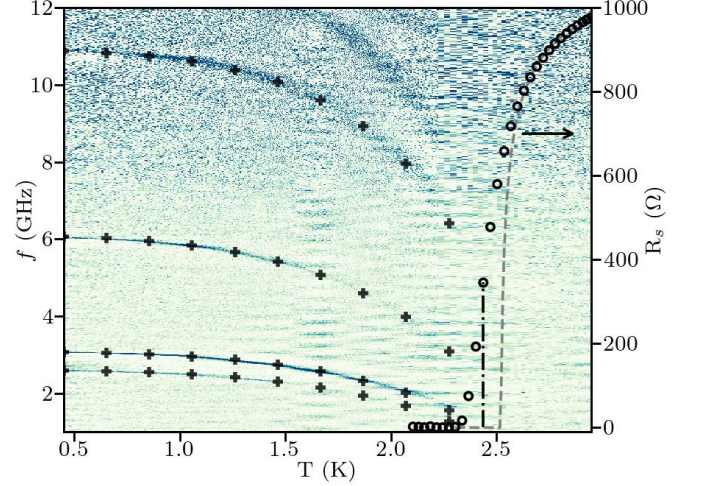


FIG. 3: (Color online) Normalized transmission spectra of the sample D, showing temperature-dependent resonances; fit of the resonances (+); temperature dependence of R_s (o); The T_c^{DC} from DC measurement is denoted by dash-dotted line and the grey dashed line is the fit of DC transition following³³. For presentation, Savitzky–Golay filter was used to suppress the background.

rical factor and suppressed T_c . Furthermore, the well-defined shape of the samples increased the quality of the resonances, showing the importance of the edges, typical for resonators. The temperature dependence of the transmission spectrum for sample D is shown in Fig. 3.

The spectrum is normalized to the normal state transmission. As it is visible, several resonances emerge from $\omega \rightarrow 0$ at T_c and with decreasing temperature, they shift toward higher frequencies. To analyze the resonances, we model them as simple capacitively-coupled resonance modes. Their temperature dependent frequency can be approximated, assuming $R \rightarrow 0$, with the LC circuit resonance equation³⁴ ($S_{21}(\omega_n) = 0$):

$$\omega_n(T) \approx \frac{1}{\sqrt{((C_r + C_c)L_r)_n + (C_r + C_c)_n L_k(\omega_n, T)}}, \quad (1)$$

where C_r and L_r are geometric parameters defining the resonance mode. Assuming these parameters are constant for the n^{th} resonance mode in the measured narrow temperature

range, the temperature dependence can be expressed by the simple equation:

$$\omega_n(T) \approx \frac{1}{\sqrt{A_n + B_n L_k(\omega_n, T)}}, \quad (2)$$

where A_n, B_n are fitting parameters, specific for each resonance mode.

The kinetic sheet inductance of a thin superconducting film with thickness much smaller than the London penetration depth is given as³⁵ $L_k(\omega, T) = \sigma_2(\omega, T)/\omega\sigma^2(\omega, T)$. The complex conductivity of the films with finite Γ are numerically calculated¹ for a set of Γ , and the full superconducting gap $\Delta_0 = \Delta(T=0)$ parameters and according to Eq. 2, the temperature dependence of the resonances in the transmission spectra are fitted, resulting in the corresponding values of Γ and Δ_0 . For MoC films, the relation $\Delta_0 = 1.84T_c$ is used²⁷ and the temperature dependence of $\Delta(T)$ follows the BCS relation.

The fitted curves for sample D are shown in Fig. 3. The estimated values of T_c and Γ resulting in the best fit, together with the expected values of Γ estimated from STS²⁷ spectra are listed in Table I. The values of Γ obtained from spectroscopy correspond reasonably to the ones obtained from STS. The estimated T_c is slightly above the values estimated from DC transport measurement, but in the broadened superconducting transition. The complex conductivity of Dynes superconductors reproduces the experimentally observed temperature dependence in the low-temperature limit, where MB conductivity model ($\Gamma \rightarrow 0$) is already saturated. As a result, the MB conductivity fit underestimates the T_c and fits the experimental dependence with several times the error of the model with finite Γ .

To further investigate the nature of the resonances, the measurement was modeled in EM software Sonnet (Fig. 1a). The calculated complex conductivity of the film was inserted into the software. The model reproduced the measurement qualitatively, showing resonant absorption dips in the transmission spectra. The resonances below 10 GHz are governed by the thin film properties. Above 10 GHz, the metal box resonances and the dielectric resonances of the substrate are present, too. The latter resonances were recognized and analyzed in Ref. 25 for experiment with thin metallic films on dielectric substrates. The kinetic inductance and geometric inductance of the metallic films are negligible in comparison to the disordered superconductors, and their resonances would be present at much higher frequencies. The high L_k of MoC films results in planar resonances present at frequencies as low as 3 GHz, despite the small dimensions of the resonator. The simulated power loss and the corresponding resonances are shown in Fig. 4. The dominant current component in the superconducting film for the first 5 resonant modes illustrates the nature of the resonances (Fig. 4). The frequencies of the resonances do not fit the experiment perfectly, partly due to the lack of experimental control in sample position limiting the accuracy of the model, and partly due to the difficulty of the simulations. However, they exhibit the same temperature dependence as in the experiment.

To conclude, we utilized a broadband transmission line flip-chip spectroscopy technique to study the superconducting

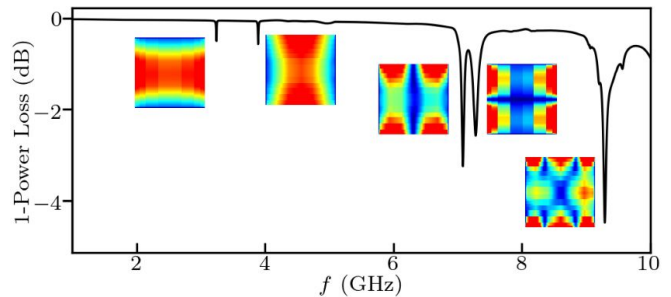


FIG. 4: (Color online) Simulated power loss in the transmission line and the corresponding eigenmodes of the planar resonator. The relative amplitude of the j_y, j_x, j_x, j_y, j_x current densities in superconducting layer are color coded.

transition of thin, strongly disordered MoC films sputtered on sapphire substrates. The spectra contained unexpected resonances, which were identified as planar resonances of the superconducting film. These resonances have low resonance frequency due to the high L_k of disordered superconductors and they correspond to the eigenmodes of the planar 2D resonator. In contrast to previous works²⁵, the dynamics of the resonances is given by the complex conductivity of the disordered films and dimensions of the films. This is further supported by the EM model in Sonnet software. The resonances were observed on rectangular $\approx 5 \times 5$ mm² films set by the substrate solely, and on optically lithographed 2.25×2.25 mm² squares with different R_s . The temperature dependence of the resonances was fitted by numerically calculated complex conductivity of disordered superconductor¹ with finite Γ . The obtained Γ parameters relate reasonably to the ones expected from STS measurements, showing that this theory could be utilized to describe the electrodynamic response of highly disordered superconductors, and vice versa: this non-contact method could be used to estimate the Γ and T_c of highly disordered films, avoiding the nontrivial calibration procedure required in similar spectroscopic techniques³⁶, or the requirement of structuring special resonators on the films³⁷. Moreover, the understanding of the nature of these resonances can help eliminate them in the required bandwidth by smart design, as for example in Ref. 38, or to utilize them as filters in sensors and QED circuitry design. Their possible advantage could be a higher power handling capability than their quasi 1D on-chip microwave counterparts³⁹ and their disjunction from the circuitry design. Finally, the bare awareness of the existence of these resonances in highly disordered films is important, as they can affect spectroscopic experiments, where strongly disordered films are studied and delicate deviations in the complex conductivity close to T_c are analyzed¹⁷.

ACKNOWLEDGMENTS

This work was supported by the Slovak Research and Development Agency under the contract APVV-16-0372, APVV-18-0358 and by the QuantERA grant SiUCs, by SAS-MTVS.

- ¹M. Žemlička, P. Neilinger, M. Trgala, M. Rehák, D. Manca, M. Grajcar, P. Szabó, P. Samuely, i. c. v. Gaži, U. Hübner, V. M. Vinokur, and E. Il'ichev, *Phys. Rev. B* **92**, 224506 (2015).
- ²G. Gol'tsman, O. Okunev, G. Chulkova, A. Lipatov, A. Dzardanov, K. Smirnov, A. Semenov, B. Voronov, C. Williams, and R. Sobolewski, *IEEE Transactions on Applied Superconductivity* **11**, 574 (2001).
- ³E. A. Tholén, A. Ergül, K. Stannigel, C. Hutter, and D. B. Haviland, *Physica Scripta* **T137**, 014019 (2009).
- ⁴B. Ho Eom, P. K. Day, H. G. LeDuc, and J. Zmuidzinas, *Nature Physics* **8**, 623 (2012).
- ⁵V. E. Manucharyan, J. Koch, L. I. Glazman, and M. H. Devoret, *Science* **326**, 113 (2009), <https://science.sciencemag.org/content/326/5949/113.full.pdf>.
- ⁶D. Niepce, J. Burnett, and J. Bylander, *Phys. Rev. Applied* **11**, 044014 (2019).
- ⁷O. V. Astafiev, L. B. Ioffe, S. Kafanov, Y. A. Pashkin, K. Y. Arutyunov, D. Shahar, O. Cohen, and J. S. Tsai, *Nature* **484**, 355 (2012).
- ⁸V. F. Gantmakher and V. T. Dolgoplov, *Physics-Uspexhi* **53**, 1 (2010).
- ⁹M. R. Beasley, J. E. Mooij, and T. P. Orlando, *Phys. Rev. Lett.* **42**, 1165 (1979).
- ¹⁰J. Krupka, M. Klinger, M. Kuhn, A. Baryanyak, M. Stiller, J. Hinken, and J. Moderski, *IEEE Transactions on Applied Superconductivity* **3**, 3043 (1993).
- ¹¹Z. Zhai, C. Kusko, N. Hakim, S. Sridhar, A. Revcolevschi, and A. Vietkine, *Review of Scientific Instruments* **71**, 3151 (2000), <https://doi.org/10.1063/1.1305519>.
- ¹²M. Scheffler, C. Fella, and M. Dressel, *Journal of Physics: Conference Series* **400**, 052031 (2012).
- ¹³C. O. M., *Nuovo Cimento* **1**, 397 (1911).
- ¹⁴J. C. Booth, D. H. Wu, and S. M. Anlage, *Review of Scientific Instruments* **65**, 2082 (1994), <https://doi.org/10.1063/1.1144816>.
- ¹⁵M. Scheffler and M. Dressel, *Review of Scientific Instruments* **76**, 074702 (2005), <https://doi.org/10.1063/1.1947881>.
- ¹⁶H. Kitano, T. Ohashi, and A. Maeda, *Review of Scientific Instruments* **79**, 074701 (2008), <https://doi.org/10.1063/1.2954957>.
- ¹⁷R. Ganguly, D. Chaudhuri, P. Raychaudhuri, and L. Benfatto, *Phys. Rev. B* **91**, 054514 (2015).
- ¹⁸F. Nabeshima, K. Nagasawa, A. Maeda, and Y. Imai, *Phys. Rev. B* **97**, 024504 (2018).
- ¹⁹H. Kitano, T. Ohashi, H. Ryuzaki, A. Maeda, and I. Tsukada, *Physica C* **412–414**, 130 (2004).
- ²⁰M. Scheffler, M. Dressel, and M. Jourdan, *J. Phys.: Conf. Ser.* **200**, 012175 (2010).
- ²¹M. Scheffler, M. Dressel, and M. Jourdan, *Eur. Phys. J. B* **74**, 331 (2010).
- ²²K. Steinberg, M. Scheffler, and M. Dressel, *Journal of Applied Physics* **108**, 096102 (2010), <https://doi.org/10.1063/1.3505706>.
- ²³D. Geiger, M. Scheffler, M. Dressel, M. Schneider, and P. Gegenwart, *J. Phys.: Conf. Ser.* **391**, 012091 (2012).
- ²⁴P. Neilinger, M. Baránek, D. Manca, and M. Grajcar, *Acta Physica Polonica A* **137**, 797 (2020).
- ²⁵M. M. Felger, M. Dressel, and M. Scheffler, *Review of Scientific Instruments* **84**, 114703 (2013), <https://doi.org/10.1063/1.4827084>.
- ²⁶R. C. Dynes, V. Narayanamurti, and J. P. Garno, *Phys. Rev. Lett.* **41**, 1509 (1978).
- ²⁷P. Szabó, T. Samuely, V. Hašková, J. Kačmarčík, M. Žemlička, M. Grajcar, J. G. Rodrigo, and P. Samuely, *Phys. Rev. B* **93**, 014505 (2016).
- ²⁸E. F. C. Driessen, P. C. J. J. Coumou, R. R. Tromp, P. J. de Visser, and T. M. Klapwijk, *Phys. Rev. Lett.* **109**, 107003 (2012).
- ²⁹P. C. J. J. Coumou, E. F. C. Driessen, J. Bueno, C. Chapelier, and T. M. Klapwijk, *Phys. Rev. B* **88**, 180505 (2013).
- ³⁰S. B. Nam, *Phys. Rev.* **156**, 470 (1967).
- ³¹F. Herman and R. Hlubina, *Phys. Rev. B* **96**, 014509 (2017).
- ³²S. J. Lee and J. B. Ketterson, *Phys. Rev. Lett.* **64**, 3078 (1990).
- ³³L. Benfatto, C. Castellani, and T. Giamarchi, *Physical Review B* **80** (2009), 10.1103/physrevb.80.214506.
- ³⁴M. Göppl, A. Fragner, M. Baur, R. Bianchetti, S. Filipp, J. M. Fink, P. J. Leek, G. Puebla, L. Steffen, and A. Wallraff, *Journal of Applied Physics* **104**, 113904 (2008).
- ³⁵J. Gao, *The Physics of Superconducting Microwave Resonators*, Ph.D. thesis, California Institute of Technology (2008).
- ³⁶M. Zinßer, K. Schlegel, M. Dressel, and M. Scheffler, *Review of Scientific Instruments* **90**, 034704 (2019), <https://doi.org/10.1063/1.5063862>.
- ³⁷L. Wendel, V. T. Engl, G. Untereiner, N. G. Ebersperger, M. Dressel, A. Farag, M. Ubl, H. Giessen, and M. Scheffler, *Review of Scientific Instruments* **91**, 054702 (2020), <https://doi.org/10.1063/1.5139986>.
- ³⁸A. Naji and P. A. Warr, *Scientific Reports* **9**, 2417 (2019).
- ³⁹P. Harvey-Collard, G. Zheng, J. Dijkema, N. Samkharadze, A. Sammak, G. Scappucci, and L. M. K. Vandersypen, *Phys. Rev. Applied* **14**, 034025 (2020).
- ⁴⁰M. Scheffler, K. Schlegel, C. Clauss, D. Hafner, C. Fella, M. Dressel, M. Jourdan, J. Sichelschmidt, C. Krellner, C. Geibel, and F. Steglich, *physica status solidi (b)* **250**, 439 (2013), <https://onlinelibrary.wiley.com/doi/pdf/10.1002/pssb.201200925>.
- ⁴¹D. C. Mattis and J. Bardeen, *Phys. Rev.* **111**, 412 (1958).
- ⁴²M. Scheffler, M. Dressel, M. Jourdan, and A. Hermann, *Nature (London)* **438**, 1135 (2005).